[Ru(xantsil)(CO)(η^6-toluene)]: Synthon for a Highly Unsaturated Ruthenium(II) Complex through Facile Dissociation of the Toluene Ligand [xantsil = (9,9-dimethylxanthene-4,5-diyl)bis(dimethylsilyl)]

Masaaki Okazaki,[†] Nobukazu Yamahira, Jim Josephus Gabrillo Minglana,[‡] Takashi Komuro, Hiroshi Ogino,[§] and Hiromi Tobita*

Department of Chemistry, Graduate School of Science, Tohoku University, Sendai 980-8578, Japan

Received November 28, 2007

The reactions of [Ru(xantsil)(CO)(η^6-$C_6H_5CH_3$)] [**1a**, xantsil = (9,9-dimethylxanthene-4,5-diyl)bis(dimethylsilyl))] with some electron-donating molecules were reported. When **1a** was dissolved in benzene, benzene replaced the η^6-toluene ligand easily at room temperature to give [Ru(xantsil)(CO)(η^6-C_6H_6)] (**1b**). The η^6-toluene ligand was also substituted by sterically less demanding two-electron donors smoothly at room temperature to afford [Ru(xantsil)(CO)L_3] (L = CH_3CN (**2**), ^{t}BuNC (**3**), and PMe_3 (**4**)). The X-ray diffraction studies revealed that they take a typical octahedral geometry, in which the xantsil ligand is coordinated to the Ru(II) center in κ^2(*Si,Si*) fashion. Reactions of **1a** with sterically demanding phosphines gave [Ru(xantsil)(CO)(PR_3)] (R = ^{i}Pr (**5**) and Cy (**6**)). According to the X-ray diffraction study, complex **6** takes a square-pyramidal geometry, in which the xantsil ligand is bound to the Ru(II) center in κ^3(*Si,Si,O*) fashion and one of the silyl groups occupies the apical position. The coordinatively unsaturated Ru(II) center is slightly stabilized by the agostic interaction by the C−H bonds in PCy_3 [Ru···H: 2.89 and 3.06 Å]. The highly coordinatively unsaturated nature in **6** was indicated by the reaction with carbon monoxide molecules to give [Ru(xantsil)$(CO)_3(PCy_3)$] (**7**) at room temperature. The typical octahedral geometry with the κ^2(*Si,Si*)-xantsil ligand was established by the X-ray diffraction study.

Introduction

Highly coordinatively unsaturated transition-metal complexes possessing 14 valence electrons are recognized as key intermediates in the homogeneous catalytic or stoichiometric reactions. In most of the reactions, the intermediates derived from oxidative addition or binding of substrates should leave adequate coordination vacancies, allowing further transformation reactions.[1] The η^6-arene-coordinated complex could be a promising candidate for such a species through the dissociation of the arene ligand. Thus, the exchange of arene molecules between free and bound states has been an important class of reactions in organometallic and surface chemistry. The arene exchange has been mechanistically investigated for late-transition-metal complexes.[2] Several possible mechanisms have been reported so far. One mechanism involves an associative process as shown in Scheme 1. An initial rearrangement of the arene from η^6- to η^4-coordination occurs to give **B**. The incoming arene coordinates with **B** in η^2-fashion to give **C**. Intramolecular rearrangement between two arene molecules, dissociation of the η^2-arene molecule, and rearrangement of the resultant arene ligand from η^4 to η^6 give **F**. Taking into account the strong σ-donor and the *trans*-influencing ability of the silyl ligands,[3] they are expected to exhibit an exceptionally strong *trans* effect. Therefore, silyl ancillary ligands would accelerate the dissociation of the η^6-arene ligand to generate highly coordinatively unsaturated intermediates. Chelate formation often stabilizes the complex, and a series of (phosphinoalkyl)silyl ligands were demonstrated to work as supporting ligands and enabled reactivity studies on their complexes.[4] Recently, we have developed a new type of bis(silyl) chelating ligand, (9,9-

Scheme 1

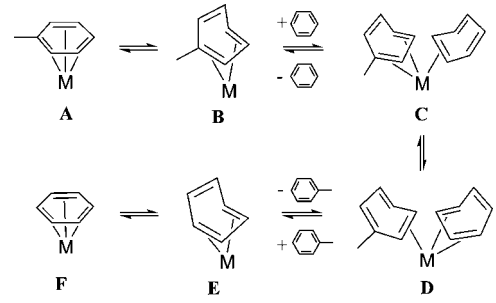

* Corresponding author. E-mail: tobita@mail.tains.tohoku.ac.jp.
[†] International Research Centre for Elements Science, Institute for Chemical Research, Kyoto University, Uji Kyoto, 611-0011, Japan.
[‡] Institute of Chemistry, University of the Philippines, Diliman, Quezon City 1101, Philippines.
[§] The Open University of Japan, Chiba, 261-8586, Japan.

(1) Crabtree, R. H. In *Activation and Functionalization of Methane*; Davies, J. A. Ed.; VCH: New York, 1990; p 69.
(2) (a) Muetterties, E. L.; Bleeke, J. R.; Sievert, A. C. *J. Organomet. Chem.* **1979**, *178*, 197. (b) Traylor, T. G.; Stewart, K. J.; Goldberg, M. J. *J. Am. Chem.Soc.* **1984**, *106*, 4445. (c) White, C.; Thompson, S. J.; Maitlis, P. M. *J. Chem. Soc., Dalton Trans.* **1977**, 1654. (d) Green, M. L. H.; Joyner, D. S.; Wallis, J. M. *J. Chem. Soc., Dalton Trans.* **1987**, 2823.
(3) (a) Chatt, J.; Eaborn, C.; Ibekwe, S. *Chem. Commun.* **1966**, 700. (b) Chatt, J.; Eaborn, C.; Ibekwe, S. D.; Kapoor, P. N. *J. Chem. Soc. A* **1970**, 1343. (c) Bentham, J. E.; Cradock, S.; Ebsworth, E. A. V. *J. Chem. Soc. A* **1971**, 587. (d) McWeeny, R.; Mason, R.; Towl, A. D. C. *Discuss. Faraday Soc.* **1969**, *47*, 20. (e) Mason, R.; Towl, A. D. C. *J. Chem. Soc. A* **1970**, 1601. (f) Hartley, F. R. *Chem. Soc. Rev.* **1973**, *2*, 163. (g) Haszeldine, R. N.; Parish, R. V.; Setchfield, J. H. *J. Organomet. Chem.* **1973**, *57*, 279. (h) Yamashita, H.; Hayashi, T.; Kobayashi, T.; Tanaka, M.; Goto, M. *J. Am. Chem. Soc.* **1988**, *110*, 4417. (i) Lichtenberger, D. L.; Rai-Chaudhuri, A. *J. Am. Chem. Soc.* **1991**, *113*, 2923. (j) Levy, C. J.; Puddephatt, R. J.; Vittal, J. J. *Organometallics* **1994**, *13*, 1559.

10.1021/om701194e CCC: $40.75
Publication on Web 02/15/2008

Scheme 2

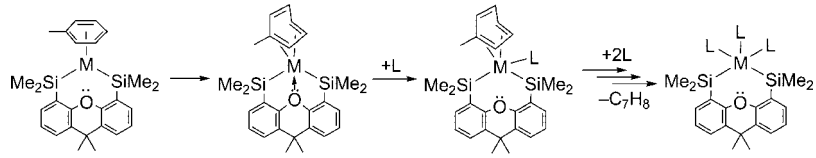

dimethylxanthene-4,5-diyl)bis(dimethylsilyl), or "xantsil".[5] In the last few decades, van Leeuwen et al. explored several diphosphine ligands having a xanthene or xanthene-like backbone and demonstrated their excellent effect on metal-catalyzed reactions based on their unique rigidity and large bite angle.[6] We applied this rigid backbone, aiming at stabilizing the bis(silyl) chelate complexes, which are easily subjected to reductive elimination, nucleophilic substitution, insertion, and so on. Another characteristic feature of xantsil is the existence of the oxygen atom, capable of coordinating to the transition metal. In the substitution reactions of the η^6-arene ligand with a two-electron donor, the intramolecular coordination of the xanthene oxygen atom would lower the activation barrier and stabilize the intermediate (Scheme 2). We report here the extremely accelerated η^6-arene substitution reactions on the [Ru(xantsil)(CO)] fragment. Structures and properties of the resulting ruthenium(II) complexes, [Ru(xantsil)(CO)L_n] [L_n = η^6-benzene, $(CH_3CN)_3$, (^{t}BuNC)$_3$, $(PMe_3)_3$, P^{i}Pr$_3$, PCy_3, $(CO)_2(PCy_3)$], will also be discussed. Some of the results reported here have appeared elsewhere in a preliminary form.[5a,d]

Results and Discussion

Facile Arene Exchange in [Ru(xantsil)(CO)(η^6-$C_6H_5CH_3$)] (1a). Extremely facile arene exchange was observed at room temperature in [Ru(xantsil)(CO)(η^6-$C_6H_5CH_3$)] (**1a**) when crystals of **1a** were dissolved in benzene to give [Ru(xantsil)(CO)(η^6-C_6H_6)] (**1b**) quantitatively (eq 1). NMR data of **1b** closely resemble those of **1a** except for the data of the η^6-benzene ligand. The ^{1}H and ^{13}C NMR signals of the η^6-benzene ligand in cyclohexane-d_{12} were observed at δ 4.98 and 97.2, respectively. The high-field shift of the signals compared to free benzene is characteristic of the η^6-arene ligands coordinated to transition metals. When the ^{1}H NMR spectrum of **1b** was measured in benzene-d_6, the signal of the coordinated benzene diminished, showing fast exchange between the η^6-benzene ligand and the benzene-d_6 solvent. The arene exchange that occurs at room temperature is sill limited and has been reported for the nickel,[7] iridium,[8] and titanium[9] systems. A series of nickel-arene complexes, [$(C_6F_5)_2$Ni(η^6-arene)], has been synthesized by a metal vapor synthetic method, in which the C_6F_5 group is essential for their isolation. The nickel-arene complexes reacted with electron-rich arenes, PEt$_3$, 1,5-cycloocatadiene, and tetrahydrofuran to afford the substitution products at room temperature. Treatment of the dimer [Ir(μ-OMe)(cod)]$_2$ with [HP^{i}Pr$_3$](BF$_4$) in acetone/benzene solution yielded the cationic arene complex [(η^6-benzene)Ir(H)$_2$(P^{i}Pr$_3$)](BF$_4$), of which the η^6-benzene ligand was readily substituted with arenes in acetone through the transient formation of [(acetone)$_3$-Ir(H)$_2$(P^{i}Pr$_3$)](BF$_4$). The reduction of TiCl$_4$ in the presence of AlCl$_3$ in benzene gave [(η^6-C_6H_6)Ti(μ-Cl)$_4$Al$_2$Cl$_4$], showing facile exchange with electron-rich arenes. Although π-arene complexes of group 8 transition metals have been of considerable interest over the last few decades, due to their high stoichiometric and catalytic activity,[10] little is known about them possessing labile π-arene ligands. Complex **1** represents the first example of a ruthenium complex that undergoes arene exchange at room temperature.

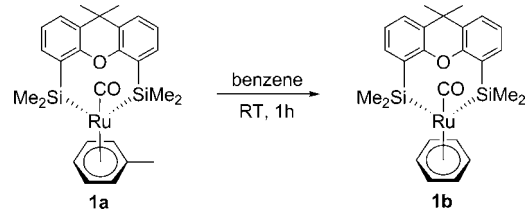

(1)

Substitution Reactions in [Ru(xantsil)(CO)(η^6-$C_6H_5CH_3$)] (1a) with Nitrile and Isonitrile. Crystals of **1a** were dissolved in acetonitrile-d_3, and the reaction was monitored by ^{1}H NMR spectroscopy. Within 30 min at room temperature, the signals assignable to **1a** diminished. Instead, the signals assignable to [Ru(xantsil)(CO)$(CD_3CN)_3$] (**2**-d_9) and free toluene were observed in the appropriate region. A large-scale experiment using acetonitrile as a solvent allowed the isolation of [Ru(xantsil)(CO)$(CH_3CN)_3$] (**2**) as colorless crystals in 98% yield

(4) (a) Stobart, S. R.; Zhou, X.; Cea-Olivares, R.; Toscano, A. *Organometallics* **2001**, *20*, 4766. (b) Brost, R. D.; Bruce, G. C.; Joslin, F. L.; Stobart, S. R. *Organometallics* **1997**, *16*, 5669, and references therein. (c) Okazaki, M.; Tobita, H.; Ogino, H. *Organometallics* **1996**, *15*, 2790. (d) Okazaki, M.; Tobita, H.; Ogino, H. *Chem. Lett.* **1997**, 437. (e) Okazaki, M.; Tobita, H.; Ogino, H. *J. Chem. Soc., Dalton Trans.* **1997**, 3531. (f) Okazaki, M.; Tobita, H.; Kawano, Y.; Inomata, S.; Ogino, H. *J. Organomet. Chem.* **1998**, *553*, 1. (g) Okazaki, M.; Ohshitanai, S.; Iwata, M.; Tobita, H.; Ogino, H. *Coord. Chem. Rev.* **2002**, *226*, 167.

(5) (a) Tobita, H.; Hasegawa, K.; Minglana, J. J. G.; Luh, L.-S.; Okazaki, M.; Ogino, H. *Organometallics* **1999**, *18*, 2058. (b) Minglana, J. J. G.; Okazaki, M.; Tobita, H.; Ogino, H. *Chem. Lett.* **2002**, 406. (c) Okazaki, M.; Minglana, J. J. G.; Yamahira, N.; Tobita, H.; Ogino, H. *Can. J. Chem.* **2003**, *81*, 1350. (d) Okazaki, M.; Yamahira, N.; Minglana, J. J. G.; Tobita, H. *Organometallics* **2004**, *23*, 4531. (e) Minglana; J. J. G.; Okazaki, M.; Hasegawa, K.; Luh, L.-S.; Yamahira, N.; Komuro, T.; Ogino, H.; Tobita, H. *Organometallics* **2007**, *26*, 5859.

(6) (a) Kranenburg, M.; van der Burgt, Y. E. M.; Kamer, P. C. J.; van Leeuwen, P. W. N. M. *Organometallics* **1995**, *14*, 3081. (b) Kranenburg, M.; Delis, J. G. P.; Kamer, P. C. J.; van Leeuwen, P. W. N. M.; Vrieze, K.; Veldman, N.; Spek, A. L.; Goubitz, K.; Fraanje, J. *J. Chem. Soc., Dalton Trans.* **1997**, 1839. (c) Buhling, A.; Kamer, C. J.; van Leeuwen, P. W. N. M.; Elgersma, J. W.; Goubitz, K.; Fraanje, J. *Organometallics* **1997**, *16*, 3027. (d) Kranenburg, M.; Kamer, P. C. J.; van Leeuwen, P. W. N. M. *Eur. J. Inorg. Chem.* **1998**, 155. (e) Goedheijt, M. S.; Reek, J. N. H.; Kamer, P. C. J.; van Leeuwen, P. W. N. M. *Chem. Commun.* **1998**, 2431. (f) Goertz, W.; Keim, W.; Vogt, D.; Englert, U.; Boele, M. D. K.; van der Veen, L. A.; Kamer, P. C. J.; van Leeuwen, P. W. N. M. *J. Chem. Soc., Dalton Trans.* **1998**, 2981. (g) van der Veen, L. A.; Boele, M. D. K.; Bregman, F. R.; Kamer, P. C. J.; van Leeuwen, P. W. N. M.; Goubitz, K.; Fraanje, J.; Schenk, H.; Bo, C. *J. Am. Chem. Soc.* **1998**, *120*, 11616.

(7) (a) Klabunde, K. J.; Anderson, B. B.; Bader, M.; Radonovich, L. J. *J. Am. Chem. Soc.* **1978**, *100*, 1313. (b) Gastinger, R. G.; Anderson, B. B.; Klabunde, K. J. *J. Am. Chem. Soc.* **1989**, *102*, 4959.

(8) (a) Torres, F.; Sola, E.; Martín, M.; López, J. A.; Lahoz, F. J.; Oro, L. A. *J. Am. Chem. Soc.* **1999**, *121*, 10632. (b) Torres, F.; Sola, E.; Martín, M.; Ochs, C.; Picazo, G.; López, J. A.; Lahoz, F. J.; Oro, L. A. *Organometallics* **2001**, *20*, 2716.

(9) Pasynkiewicz, S.; Ciezyński, R.; Dzierzgowski, S. *J. Organomet. Chem.* **1973**, *54*, 203.

(10) (a) Bennett, M. A. In *Comprehensive Organometallic Chemistry II*; Abel, E. W., Stone, F. G., Wilkinson, G., Eds.; Pergamon: New York, 1995; Vol. 7, p 549. (b) Gimeno, J.; Cadierno, V.; Crochet, P. In *Comprehensive Organometallic Chemistry III*; Crabtree, R. H., Mingos, D. M. P., Eds.; Pergamon: New York, 2007; Vol. 6, p 531.

Scheme 3. Synthesis of [Ru(xantsil)(CO)L_3] (L = CH_3CN (2), ^{t}BuNC (3))[a]

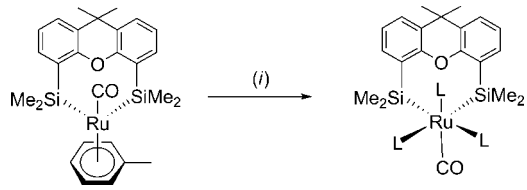

[a] (*i*) L = CH_3CN: acetonitrile, RT, 30 min; L = ^{t}BuNC: + ^{t}BuNC, cyclohexane, RT, immediately.

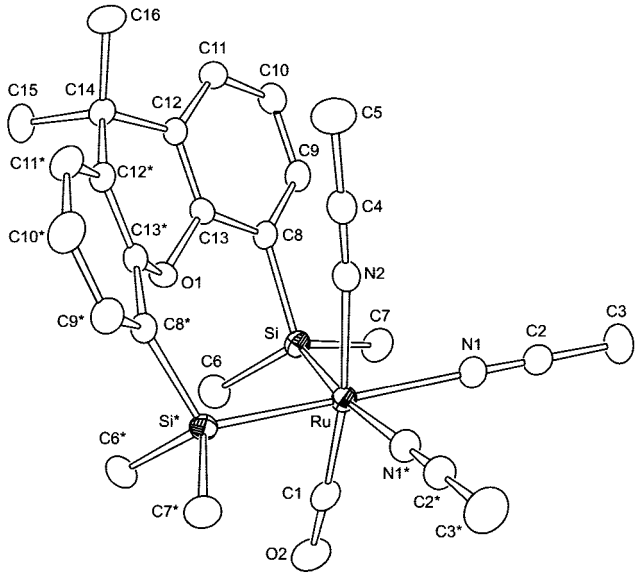

Figure 1. ORTEP drawing of **2**. Thermal ellipsoids are drawn at the 50% probability level, and hydrogen atoms are omitted for clarity. Selected bond lengths (Å) and angles (deg): Ru−Si 2.3960(5), Ru−N1 2.2010(16), Ru−N2 2.119(2), Ru−C1 1.813(3), Si−Ru−Si* 96.17(2), C1−Ru−N1 101.28(7), C1−Ru−N2 170.73(9), N1−Ru−N2 85.50(5), N1−Ru−N1* 84.96(8), C1−Ru−Si 82.87(5), N2−Ru−Si 90.97(4), N1−Ru−Si 89.34(4), N1−Ru−Si* 173.51(4). Asterisks indicate atoms generated by the symmetry operation (x, $-y + 1/2$, z).

(Scheme 3). Elemental analysis established the formula of **2**. The infrared (IR) spectrum shows three bands at 2362, 2336, and 1916 cm^{-1}. The first two are assignable to the CN stretching vibration mode of three acetonitrile ligands. The last one is assignable to the CO stretching vibration mode, and the wavenumber is very close to that in **1a** (1913 cm^{-1}). The $^{29}Si\{^1H\}$ NMR spectrum shows a singlet signal at δ 13.2, and the chemical shift lies in the typical range expected for silylruthenium(II) complexes.[11]

The molecular structure of **2** was determined by X-ray analysis (Figure 1). The molecule exhibits a mirror plane including Ru, O1, and C14 atoms. Complex **2** takes a slightly distorted octahedral geometry in which three incoming acetonitrile ligands occupy the *fac*-geometry, as suggested by the IR data. The interatomic distance of Ru−O1 is 3.563(2) Å, indicating no direct interaction between them. The Ru−Si bond distance [2.3960(5) Å] is within the range of those in related silylruthenium(II) complexes. In general, both silyl and carbonyl ligands exhibit high *trans* influence, and the former is estimated to be higher than the latter. Accordingly, the bond distances of Ru−N1 and Ru−N1* (2.2010(16) Å) are significantly longer than that of Ru−N2 (2.119(2) Å), and both are considerably longer than the average Ru−N bond distances in acetonitrile-coordinated ruthenium complexes [2.05 Å]. The xanthene core is bent, and the dihedral angle between the least-squares planes of the two aromatic rings is 31.03(6)°.

The toluene ligand in **1a** was easily substituted by three ^{t}BuNC molecules in cyclohexane at room temperature to give [Ru(xantsil)(CO)(CN^tBu)$_3$] (**3**) in 82% yield [Scheme 3]. The ^1H NMR spectrum of **3** shows two kinds of singlets for the CN^tBu ligands at δ 0.44 (9H) and 1.02 (9H × 2). The former, located at the *trans* position of CO, appears at higher field probably due to the ring current of the xanthene arene rings. The signals for $SiMe_2$ and 9,9-CMe_2 are observed at δ 1.05 and 1.28 and δ 1.54 and 1.67, respectively. The $^{13}C\{^1H\}$ NMR signals can also be assigned in a similar way. The $^{29}Si\{^1H\}$ NMR spectrum shows a signal at δ −4.6, characteristic of the silyl-ruthenium(II) complexes. In the IR spectrum, in addition to the ν_{CO} band at 1927 cm^{-1}, three strong-intensity bands of ν_{CN} are observed at 2127, 2137, and 2170 cm^{-1}. The wavenumber is indicative of their linear coordination mode.[12] Complex **3** is very stable in air even in solution, reflecting the rigid coordination of three isonitrile ligands to the Ru(II) center. A tentative X-ray structure analysis of **3** revealed the structure, in which three isonitirle ligands take a *fac*-geometry and one of them faces the xanthene core (see the Supporting Information).

Substitution Reactions in [Ru(xantsil)(CO)(η^6-$C_6H_5CH_3$)] (1a) with Tertiary Phosphines. We examined the reactions of **1a** with some tertiary phosphines. The η^6-toluene ligand was substituted by three PMe_3 molecules in dichloromethane at room temperature to give [Ru(xantsil)(PMe_3)$_3$(CO)] (**4**) in 84% yield (eq 2). The molecular structure of **4** was unequivocally determined by an X-ray diffraction study (Figure 2).[5d] Complex **4** takes a slightly distorted octahedral geometry, in which three incoming PMe_3 ligands occupy the *fac*-positions. In contrast to **2** and **3**, the carbonyl ligand faces the xanthene core to avoid the steric repulsion between the bulkier PMe_3 and the xanthene moiety. The ruthenium−silicon bonds [Ru−Si1 (2.5276(8) Å) and Ru−Si2 (2.5234(8) Å)] are unusually long, which can be explained by the steric requirement of the xantsil ligand, which is enhanced by three bulky PMe_3 ligands: That is, the rigid xanthene core forces two methyl groups (C3 and C4) to be within an extremely short interatomic distance (3.224(6) Å) compared to the sum of the effective van der Waals radii of two methyl groups (4.0 Å). The steric repulsion causes the other methyl groups (C2 and C5) on the silicon atoms to move closer to the methyl groups on the P2 and P3 phosphines (C2···C25 3.250(5) Å, C5···C28 3.298(5) Å), leading to considerable stretching of the ruthenium−silicon bonds.

The high *trans* effect of the xantsil ligand and steric repulsion between the xantsil and PMe_3 ligands mentioned above are reflected in the extremely high lability of the PMe_3 ligands (eq 3). Even in a poorly coordinating solvent such as dichloromethane, an equilibrium is achieved instantaneously between **4** and **4′** through the dissociation of one of the PMe_3 ligands. This is supported by the observation that when colorless crystals of **4** were dissolved in CD_2Cl_2, the solution turned yellow and the ^1H NMR spectrum exhibited several signals assignable to

(11) (a) Eisen, M. S. In *The Chemistry of Organic Silicon Compounds*; Rappoport, Z., Apeloig, Y., Eds.; Wiley: New York, 1998; Vol. 2, Chapter 35, pp 2037–2128. (b) Tilley, T. D. In *The Silicon-Heteroatom Bond*; Patai, S., Rappoport, Z., Eds.; Wiley: New York, 1991; Chapters 9, 10, pp 245–308, pp 309–364.

(12) Cotton, E. A.; Wilkinson, G. In *Advanced Inorganic Chemistry*, 5th ed.; Wiley: New York, 1988; p 256.

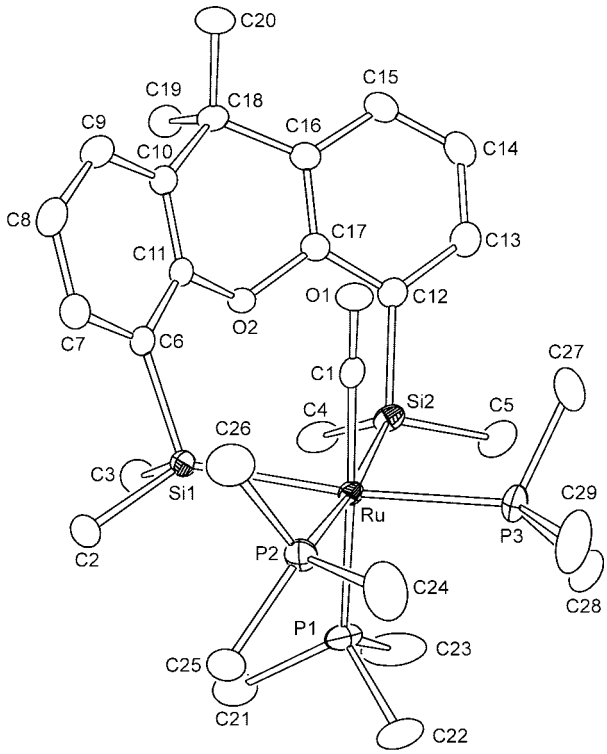

Figure 2. ORTEP drawing of **4**. Thermal ellipsoids are drawn at the 50% probability level, and hydrogen atoms are omitted for clarity. Selected bond lengths (Å) and angles (deg): Ru−P1 2.4004(8), Ru−P2 2.4003(8), Ru−P3 2.3930(8), Ru−Si1 2.5276(8), Ru−Si2 2.5234(8), Ru−C1 1.864(3), P1−Ru−P2 93.80(3), P2−Ru−P3 97.14(3), P3−Ru−P1 93.37(3), P1−Ru−Si1 92.31(3), P1−Ru–Si2 91.51(3), P2−Ru−Si1 85.09(3), P2−Ru−Si2 173.54(3), P3−Ru−Si1 173.74(3), P3−Ru−Si2 86.22(3), Si1−Ru−Si2 91.02(3), C1−Ru−P1 174.88(9), C1−Ru−P2 90.12(9), C1−Ru−P3 89.41(9), C1−Ru−Si1 84.73(8), C1−Ru−Si2 84.38(9).

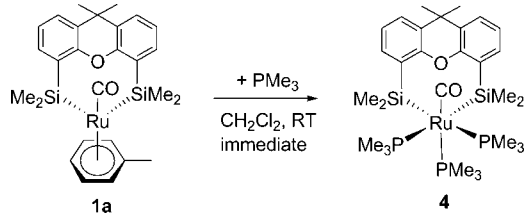

(2)

resonances of **4′** and a broad signal of free PMe_3 in addition to the signals of **4**. No signal was observed in the high-field region characteristic of the Ru−H moiety. In the $^{31}P\{^1H\}$ NMR spectrum, three new broad signals were observed at δ −59.4, −6.5, and 27.4. The first signal was assigned to the dissociated PMe_3, while the last two were assigned to **4′**. Furthermore, addition of excess PMe_3 to the yellow solution shifted the equilibrium in eq 3 to the left to form **4** predominantly, causing the yellow color to disappear. These results are consistent with the formula of **4′** as [Ru(xantsil)(CO)$(PMe_3)_2$].

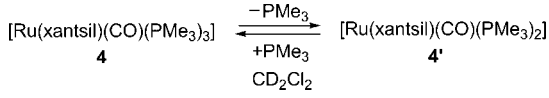

(3)

To clarify the geometry of **4′**, the geometry of [Ru(xantsil)-(CO)$(PMe_3)_2$] was optimized by DFT calculations (Figure 3, Table 2). Three intermediates were identified as stationary points on the potential energy surface. Dissociation of a PMe_3 ligand located at the *trans* position of the silyl groups would be accelerated by their strong *trans* effect, giving **4a**. Thus, **4a** takes a square-pyramidal geometry with the silyl group (Si1) in the apical position. Isomerization between the pentacoordinated **4a** and **4b** seems facile. Subsequent intramolecular coordination of the xanthene oxygen atom gives **4c** with 18 valence electrons. The interatomic distance of Ru−O1 (2.300 Å) in **4c** is significantly shorter than those in **4a** (3.671 Å) and **4b** (3.351 Å) and lies in the range expected for the Ru−O dative bonds. Complex **4c** is lowest in energy among three optimized forms. The geometry with two chemically inequivalent PMe_3 ligands is consistent with the $^{31}P\{^1H\}$ NMR spectroscopic data. In the dissociation of the PMe_3 ligand, coordination of the intramolecular oxygen atom in xantsil would be crucial to lower the activation barrier and stabilize the intermediate.

The reaction of **1a** with 5 equiv of P^iPr_3 in dichloromethane-d_2 was monitored by NMR spectroscopy (eq 4). After 10 min at room temperature, an equilibrium was attained between **1a**, [Ru(xantsil)(CO)(P^iPr_3)] (**5**), toluene, and P^iPr_3 through the dissociation of the η^6-toluene ligand, followed by the intramolecular coordination of the xanthene oxygen atom (vide infra). The molar ratio of **1a** and **5** was estimated to be 1.0:1.6 based on the intensity of the ^1H NMR signals. Addition of 20 equiv of P^iPr_3 shifted the equilibrium to the right side (**1a**:**5** = 1.0:9.1), although isolation of **5** was not achieved due to instability. Complex **5** was uniquely characterized by comparison of the NMR data with **6** (vide infra).

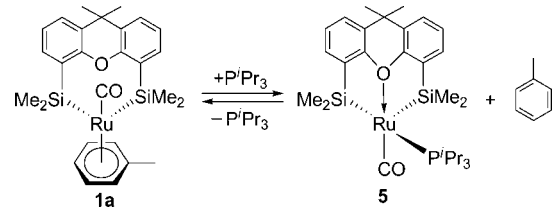

(4)

Treatment of **1a** with a bulkier PCy_3 (5 equiv) gave [Ru(xantsil)(CO)(PCy_3)] (**6**) in 76% yield (eq 5). The molecular structure was fully characterized by an X-ray diffraction study and consistent with the prediction by the DFT calculations (Figure 4).[5d] A characteristic feature of **6** is the intramolecular coordination of the oxygen atom in xantsil. The Ru−O1 distance of 2.268(4) Å is within the range expected for the ruthenium(II)−oxygen dative bonds and close to that in [Ru{κ^2(*Si,Si*)-$SiMe_2O(Me)SiMe_2$}(H){κ^3(*Si,Si,O*)-xantsil)}(CO)] [2.289(8) Å].[5c] Thus, complex **6** takes a distorted square-pyramidal geometry with the strongly electron-releasing silyl group of xantsil (Si1) in the apical position. The coordinatively unsaturated ruthenium center is stabilized by a weak agostic interaction of the C−H bonds in the cyclohexyl group [Ru−H15 = 2.89 Å, Ru−H22 = 3.06 Å] (Figure 5).

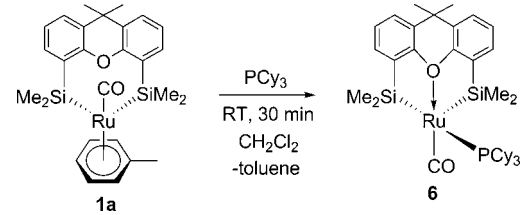

(5)

In the ^1H NMR spectrum, four signals due to methyl groups appear at δ 0.20 (6H, SiMe), 0.51 (6H, SiMe), 1.51 (3H,

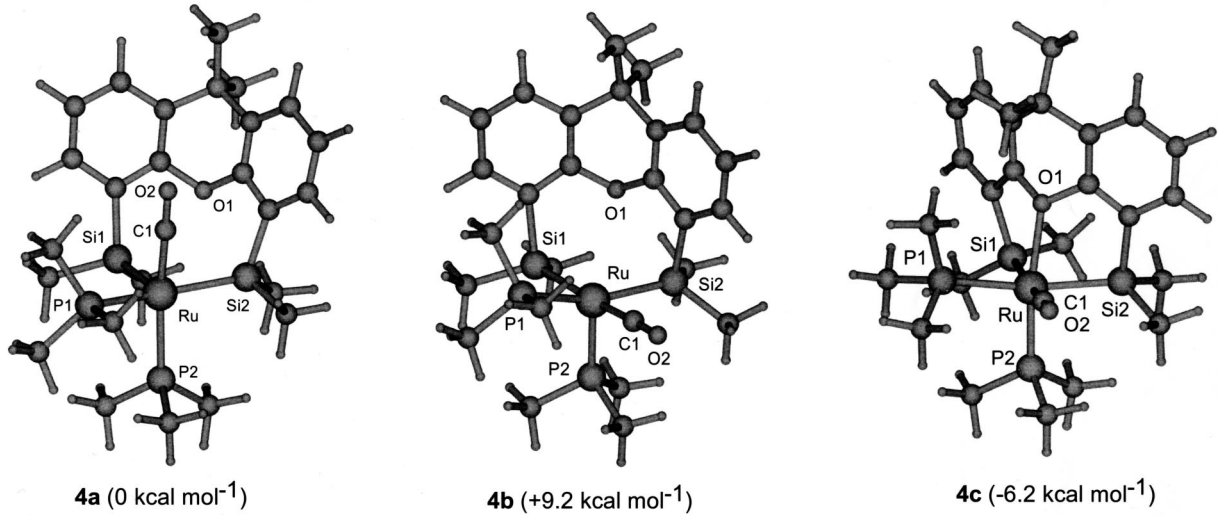

Figure 3. Optimized structures of [Ru(xantsil)(PMe_3)$_2$(CO)] by the DFT calculation (B3LYP) with the use of a basis set, i.e., SDD for Ru, 6-31G(d) for Si and P, and 6-31G for the rest.

Table 1. Crystallographic Data of 2·CH_3CN, 4, 6, 8·CH_2Cl_2, and 9

	2·CH_3CN	4	6	8·CH_2Cl_2	9
formula	$C_{22}H_{30}N_4ORuSi_2$	$C_{29}H_{51}O_2P_3RuSi_2$	$C_{38}H_{57}O_2PRuSi_2$	$C_{41}H_{59}Cl_2O_4PRuSi_2$	$C_{40}H_{48}O_4Ru_2Si_4$
cryst size (mm)	0.40 × 0.40 × 0.10	0.25 × 0.20 × 0.20	0.10 × 0.10 × 0.05	0.25 × 0.20 × 0.10	0.30 × 0.10 × 0.10
fw	617.86	681.86	734.06	875.00	907.28
cryst syst	orthorhombic	orthorhombic	triclinic	monoclinic	triclinic
space group	*Pnma*	*Pbca*	$P\bar{1}$	$P2_1/c$	$P\bar{1}$
a (Å)	22.3683(7)	17.0553(4)	10.1305(17)	15.9513(5)	10.3381(4)
b (Å)	14.0012(3)	20.1437(6)	10.3795(12)	10.5822(3)	10.4244(6)
c (Å)	9.5533(2)	19.2039(6)	19.2411(18)	25.8317(10)	10.4263(5)
α (deg)	90	90	98.116(4)	90	93.4825(14)
β (deg)	90	90	92.896(6)	101.3523(10)	115.9243(10)
γ (deg)	90	90	112.966(8)	90	109.649(3)
V (Å^3)	2991.93(13)	6597.6(3)	1831.7(4)	4275.1(2)	922.65(8)
Z	4	8	2	4	1
F_{000}	1280	2864	776	1832	464
μ(Mo Kα) (mm^{-1})	0.635	0.718	0.569	0.624	0.991
no. of reflns collected	21 810	47 454	16 127	31 960	8263
no. of indep reflns (R_{int})	3355 (0.0301)	7552 (0.0525)	8050 (0.0551)	9549 (0.0369)	4155 (0.0609)
max. and min. transmn	0.94 and 0.79	0.93 and 0.84	0.95 and 0.95	0.94 and 0.86	0.91 and 0.76
absorp corr	numerical	numerical	empirical	numerical	numerical
no. of data/restrains/params	3353/0/194	7552/0/349	8050/0/403	9549/0/466	4155/0/232
R_1, wR_2 [$I > 2\sigma(I)$]	0.0273, 0.0653	0.0415, 0.1011	0.0594, 0.1702	0.0420, 0.1350	0.0420, 0.1175
R_1, wR_2 [all data]	0.0287, 0.0660	0.0525, 0.1280	0.0830, 0.2028	0.0520, 0.1698	0.0491, 0.1265
GOF	1.195	1.226	1.165	1.174	1.155
largest diff peak and hole (e Å^{-3})	0.439 and −0.549	0.625 and −1.1015	0.888 and −1.831	1.618 and −2.425	0.813 and −0.807

9-CMe), and 1.80 (3H, 9-CMe). No signals were observed in the high-field region typical for the metal-hydrido moiety. The $^{29}Si\{^1H\}$ NMR spectrum exhibits only a doublet signal at δ 48.6 coupled with one ^{31}P nuclei (J_{SiP} = 39.0 Hz). These spectroscopic features can be explained by assuming facile flipping of the PCy_3 ligand as illustrated in Scheme 4. Kira et al. observed the related dynamic behavior of [(Cy_3P)Pd-$\{(R_3Si)_2Si{=}Si(SiR_3)_2\}$] and estimated the symmetrical (Y-type) transition state for the flipping.[13] The $^{31}P\{^1H\}$ NMR spectrum shows a signal at δ 25.0. The IR spectrum includes a strong bond at 1876 cm^{-1} assigined to the ν_{CO} band.

Complex **6** can be a good synthon for the facile generation of a coordinatively unsaturated ruthenium(II) complex bearing 14 valence electrons through dissociation of the xanthene oxygen atom.[14] The coordinative unsaturation of **6** was indicated by the reaction with CO (Scheme 5). A dichloromethane solution of **6** was stirred at room temperature for 1 h under a CO atmosphere. Workup of the reaction mixture gave a white solid of [Ru(xantsil)$(CO)_3(PCy_3)$] (**8**) in 84% yield. Recrystallization from CH_2Cl_2/hexane gave colorless crystals of **8** suitable for X-ray diffraction study (Figure 6).[5d] Complex **8** adopts a slightly distorted octahedral geometry in which three carbonyl ligands are located in a *mer*-relationship. Accordingly, the interatomic distance of Ru−O1 [3.581(2) Å] indicates no interaction between them.

The variable-temperature NMR study on the CD_2Cl_2 solution of **8** clearly indicated the existence of fluxional behavior. At 230 K, the Si−Me groups on xantsil shows four signals, which

(13) Kira, M.; Sekiguchi, Y.; Iwamoto, T.; Kabuto, C. *J. Am. Chem. Soc.* **2004**, *126*, 12778.

(14) (a) Ogasawara, M.; Huang, D.; Streib, W. E.; Huffman, J. C.; Gallego-Planas, N.; Maseras, F.; Eisenstein, O.; Caulton, K. G. *J. Am. Chem. Soc.* **1997**, *119*, 8642. (b) Huang, D.; Streib, W. E.; Bollinger, J. C.; Caulton, K. G.; Winter, R. F.; Scheiring, T. *J. Am. Chem. Soc.* **1999**, *121*, 8087. (c) Baratta, W.; Herdtweck, E.; Rigo, P. *Angew. Chem., Int. Ed.* **1999**, *38*, 1629. (d) Carmona, D.; Vega, C.; Lahoz, F. J.; Atencio, R.; Oro, L. A.; Lamata, M. P.; Viguri, F.; SanJose, E. *Organometallics* **2000**, *19*, 2281. (e) Sanford, M. S.; Henling, L. M.; Day, M. W.; Grubbs, R. H. *Angew. Chem., Int. Ed.* **2000**, *39*, 3451. (f) Watson, L. A.; Ozerov, O. V.; Pink, M.; Caulton, K. G. *J. Am. Chem. Soc.* **2003**, *125*, 8426.

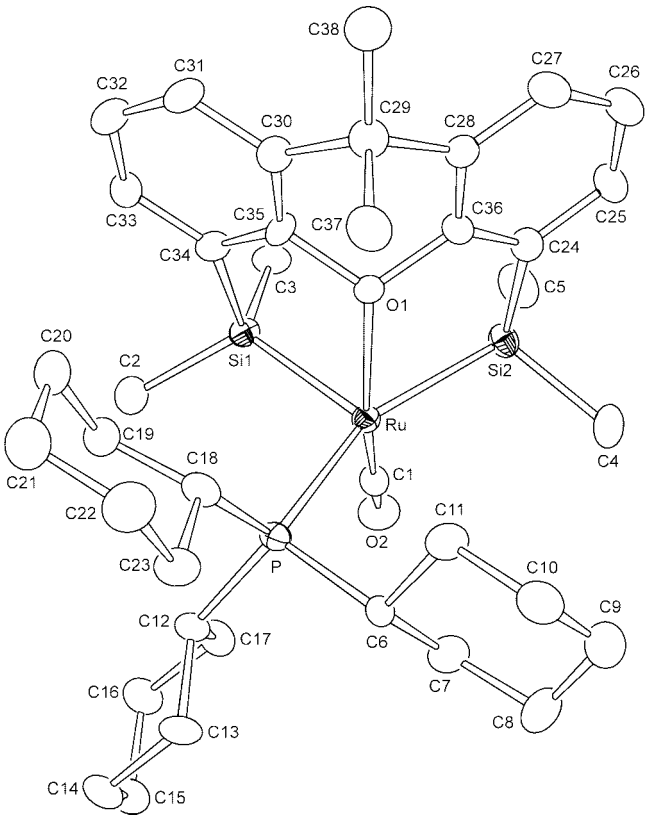

Figure 4. ORTEP drawing of **6**. Thermal ellipsoids are drawn at the 50% probability level, and hydrogen atoms are omitted for clarity. Selected bond lengths (Å) and angles (deg): Ru−C1 1.803(6), Ru−O1 2.268(4), Ru−Si1 2.2870(16), Ru−Si2 2.3584(16), Ru−P 2.4522(15), C1−Ru−O1 158.9(2), C1−Ru−Si1 87.8(2), O1−Ru−Si1 82.05(11), C1−Ru−Si2 83.0(2), O1−Ru−Si2 81.31(11), Si1−Ru−Si2 102.97(6), C1−Ru−P 103.7(2), O1−Ru−P 96.62(11), Si1−Ru−P 102.08(6), Si2−Ru−P 154.30(6).

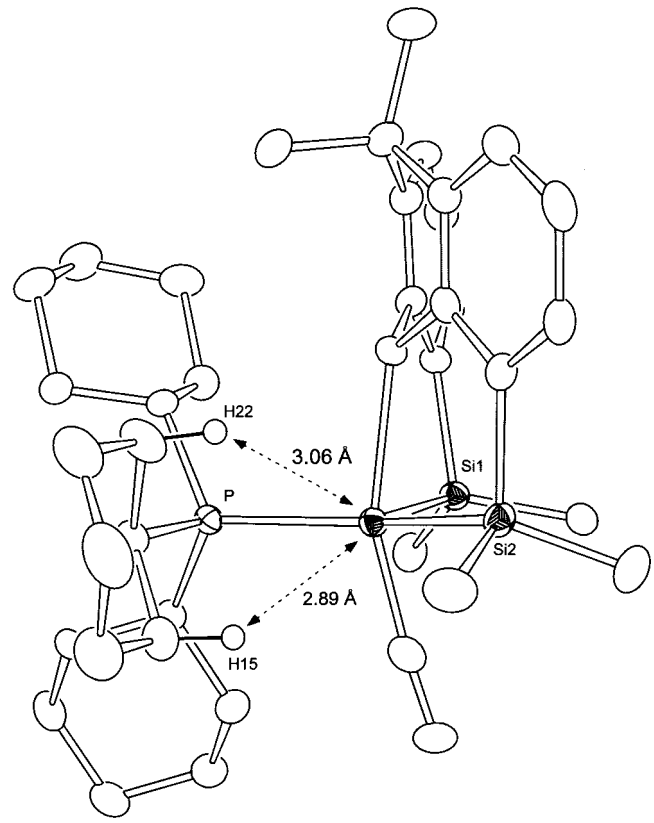

Figure 5. Agostic interactions between the Ru(II) center and cyclohexyl groups on PCy_3.

Scheme 4. Flipping of PCy_3 on the Ru(xantsil)(CO) Fragment

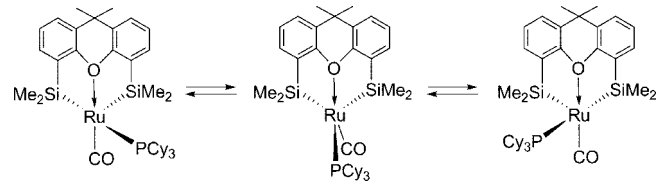

Scheme 5

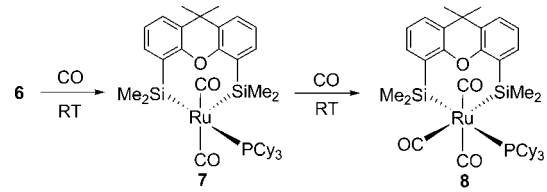

is consistent with the X-ray crystal structure. On warming, the signals at δ 0.64 and 0.72 coalesce at 270 K [$\Delta\nu$ (at 230 K) = 26.6 Hz], and those at δ 0.46 and 0.66 at 286 K [$\Delta\nu$ (230 K) = 61.1 Hz]. Finally, they become two singlet signals at room temperature. From the data, the barriers for two exchange process of Si−Me groups were calculated by the coalescence point method to be $\Delta G^{\ddagger}_{270} = 57.7$ kJ mol^{-1} and $\Delta G^{\ddagger}_{286} = 56.2$ kJ mol^{-1}, respectively. A likely process is the inversion of the puckered chelate ring (Scheme 6). Such a fluxional behavior was also observed in **1**, and the activation barrier of $\Delta G^{\ddagger}_{240} =$ 47 kJ mol^{-1} was almost the same as that in **8**. The $^{31}P\{^1H\}$ NMR spectrum shows a singlet signal at δ 39.3. The $^{29}Si\{^1H\}$ NMR spectrum at 230 K exhibits two doublet signals at δ −6.2 ($J_{PSi} = 45.1$ Hz) and −2.2 ($J_{PSi} = 8.8$ Hz), where the former is assigned to the silicon atom *trans* to PCy_3 and the latter to that *trans* to CO based on the coupling constants of J_{PSi}. The IR spectrum in CD_2Cl_2 contains three strong-intensity bands at 2040, 1992, and 1946 cm^{-1}, characteristic of the *mer*-relationship of three carbonyl ligands.

The reaction of **6** with CO was monitored spectroscopically (Scheme 5). Introduction of CO gas into an NMR tube containing the CD_2Cl_2 solution of **6** at room temperature caused the solution to turn from orange to dark green and then finally colorless. Accordingly, the $^{31}P\{^1H\}$ NMR spectrum indicated the existence of the intermediate **7** (δ 37.6), which was subsequently converted to the single product **8** (δ 39.3). The *trans* geometry of two carbonyl ligands in **7** is clearly supported by the IR spectrum: The intensity of the symmetric vibration at 2036 cm^{-1} is quite weak, while that of the asymmetric vibration at 1927 cm^{-1} is strong. In the $^{29}Si\{^1H\}$ NMR spectrum, except the signals for **6** and **8**, a new doublet signal was observed at δ 21.8 coupled with the ^{31}P nuclei ($^2J_{PSi} =$ 23.2 Hz) that was attributable to **7**. On the basis of these spectroscopic data, complex **7** is likely to take a square-pyramidal geometry with the silyl group in the axial position, which exhibits dynamic behavior including flipping of the PCy_3 ligand as in **6**.

Thermolysis of [Ru(xantsil)(CO)(η^6-$C_6H_5CH_3$)] (1a) in the Absence of Donor Molecules. When **1a** was heated in *n*-decane at 140 °C for 1 day in the absence of donor molecules, the dimer [Ru(xantsil)(CO)]$_2$ (**9**) was obtained as yellow crystals in 73% yield. No NMR spectroscopic data were obtained for **9** due to its poor solubility in organic solvents. A strong band at 1917 cm^{-1} in the IR spectrum confirms the presence of CO,

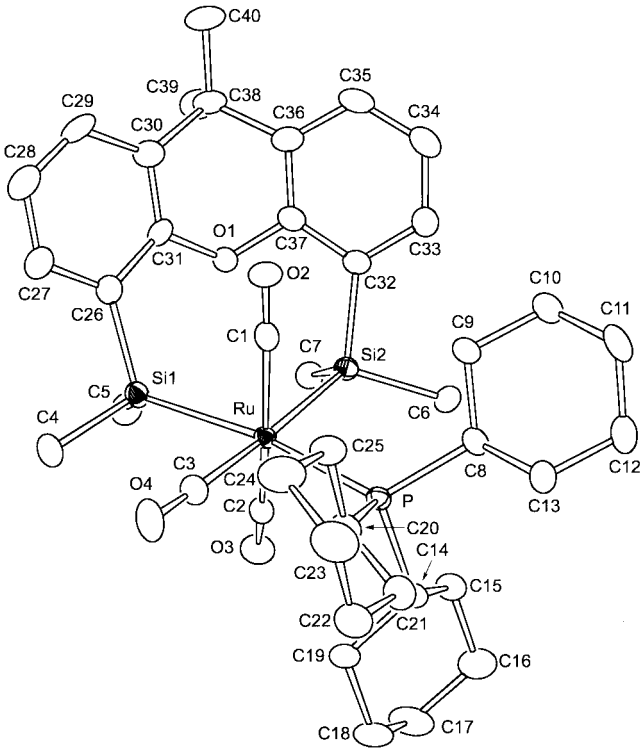

Figure 6. ORTEP drawing of **8**. Thermal ellipsoids are drawn at the 50% probability level, and hydrogen atoms are omitted for clarity. Selected bond lengths (Å) and angles (deg): Ru−C1 1.934(4), Ru−C2 1.913(4), Ru−C3 1.928(4), Ru−P 2.4935(8), Ru−Si1 2.5366(9), Ru−Si2 2.5730(9), C1−Ru−C2 159.89(14), C1−Ru−C3 95.72(15), C2−Ru−C3 99.33(15), C1−Ru−P 96.25(10), C2−Ru−P1 97.90(10), C3−Ru−P 86.53(10), C1−Ru−Si1 85.88(10), C2−Ru−Si1 83.27(10), C3−Ru−Si1 81.43(10), C1−Ru−Si2 83.99(10), C2−Ru−Si2 80.05(10), C3−Ru−Si2 175.93(11), P−Ru−Si1 167.93(3), P−Ru−Si2 97.54(3), Si1−Ru−Si2 94.50(3).

Scheme 6. Inversion of the Puckered Xanthene Chelate Ring in 8

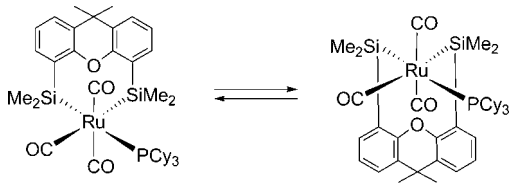

and the value is comparable to that in **1a** (1913 cm^{-1}). A weak peak of M^+ was observed at *m*/*z* 908 in the mass spectrum (EI).

The structure of **9** was unequivocally determined by an X-ray diffraction study (Figure 7). Complex **9** is proven to be a dimer in which one of the arene rings of xantsil is coordinated to the ruthenium atom in a η^6-fashion. The structure is essentially the same as **1a** except that a Ru(xantsil)(CO) moiety replaces the η^6-toluene as the η^6-coordinated ligand. The ruthenium atom is bound equivalently to the six carbon atoms of the xanthene arene rings. The aryl C−C bond lengths of the η^6-coordinated xantsil moiety range from 1.403(5) to 1.428(5) Å, while the aryl C−C bond lengths in the noncoordinated moiety range from 1.384(5) to 1.399(5) Å. The Si1−Ru−Si2 angle of 95.26(3)° is almost the same as that in **1a** [94.81(6) Å]. There is no direct interaction between the two ruthenium atoms (Ru−Ru* 4.794 Å).

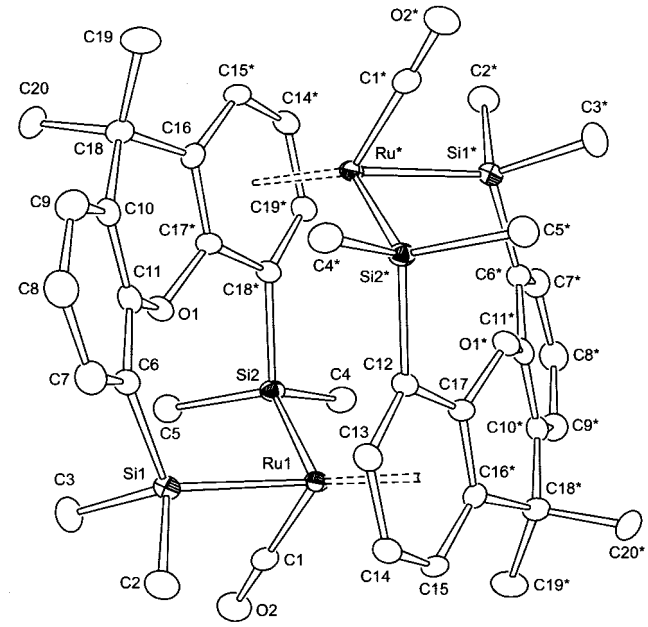

Figure 7. ORTEP drawing of **9**. Thermal ellipsoids are drawn at the 50% probability level, and hydrogen atoms are omitted for clarity. Selected bond lengths (Å) and angles (deg): Ru−C1 1.818(4), Ru−C12 2.392(3), Ru−C13 2.288(4), Ru−C14 2.272(4), Ru−C15 2.251(3), Ru−C16* 2.415(3), Ru−C17 2.458(3), Ru−Si1 2.4392(10), Ru−Si2 2.4321(10), C6−C7 1.399(5), C7−C8 1.394(6), C8−C9 1.391(6), C9−C10 1.392(5), C10−C11 1.384(5), C11−C6 1.393(5), C12−C13 1.417(5), C13−C14 1.422(5), C14−C15 1.407(5), C15−C16* 1.428(5), C16*−C17 1.403(5), C17−C12 1.416(5), C1−Ru−Si1 81.40(12), Si1−Ru−Si2 95.26(3), C1−Ru−Si2 79.49(12). Asterisks indicate atoms generated by the symmetry operation (−*x*, −*y*, −*z*).

Conclusion

The η^6-toluene ligand in [Ru(xantsil)(η^6-toluene)(CO)] (**1a**) can be readily replaced with an arene or some two-electron donor ligands under mild conditions. The substitution products also exhibit high lability through dissociation of the incoming ligands. The exceptionally high lability in the xantsil-ruthenium(II) system is attributable to (i) strong trans effect of two silyl groups, (ii) steric requirement of the xantsil leading to the severe repulsion between the $SiMe_2$ parts of xantsil and the outgoing ligands, and (iii) intramolecular coordination of the xantsil oxygen atom leading to stabilization of the transition state and/or intermediate. Considering the high lability of the η^6-toluene ligand, complex **1a** could become a synthetic equivalent of the Ru(II) species with 12 or 14 valence electrons depending on the coordination of the xanthene oxygen atom. Such a highly coordinatively unsaturated species is expected to show higher catalytic activity than the corresponding 16-electron species due to the presence of two or three easily accessible, low-lying empty orbitals that can be used in the reactions involving successive binding of substrates, oxidative addition, σ-bond metathesis, migration, etc.

Experimental Section

General Procedures. All manipulations were carried out under a dry nitrogen atmosphere. Hexane and benzene were distilled from sodium-benzophenone ketyl and dichloromethane and acetonitrile from calcium hydride immediately prior to use. Benzene-d_6 and cyclohexane-d_{12} were dried over a potassium mirror and dichloromethane-d_2 and acetonitrile-d_3 over molecular sieves 3 and 4 Å,

respectively. They were transferred into an NMR tube under vacuum. [Ru(xantsil)(CO)(η⁶-toluene)] (**1a**) was prepared according to the literature method.[5a,e] Other chemicals were purchased and used as received.

Physical Measurements. NMR spectra were obtained at room temperature unless otherwise indicated on a Bruker ARX-300 or AV-300 spectrometer. ^{1}H, ^{13}C{^{1}H}, and ^{29}Si{^{1}H} NMR spectra were recorded at 300, 75.5, and 59.6 MHz, respectively, and referenced to $SiMe_4$. ^{31}P{^{1}H} NMR spectra were recorded at 121.5 MHz and referenced to 85% aqueous H_3PO_4. ^{29}Si{^{1}H} NMR spectra were obtained by a DEPT pulse sequence. IR spectra were recorded on a Horiba FT-730 spectrometer. Mass spectra were measured using a JEOL JMS-HX110 or Hitachi M2500S spectrometer.

Reaction of [Ru(xantsil)(CO)(η⁶-toluene)] (1a) with Benzene. Colorless crystals of **1a** (10.0 mg, 0.0183 mmol) were dissolved in benzene (5 mL). After stirring for 3 h at room temperature, the solution was evaporated to dryness to give an analytically pure sample of [Ru(xantsil)(CO)(η⁶-C_6H_6)] (**1b**) as a white powder. Yield: 9.7 mg (100%). Anal. Calcd for $C_{26}H_{30}O_2Si_2Ru$: C, 58.73; H, 5.69. Found: 58.56; H, 5.89. MS (FAB, *m*-nitrobenzyl alcohol): *m*/*z* 532 (M^+, 22), 454 (M^+ − benzene, 100). ^{1}H NMR (300 MHz, C_6D_{12}): δ 0.57, 0.64 (s, 6H × 2, $SiMe_2$), 1.39, 1.78 (s, 3H × 2, 9,9′-CMe_2), 4.98 (s, 6H, η⁶-C_6H_6), 7.00–7.26 (m, 6H, xanthene). ^{13}C{^{1}H} NMR (75.5 MHz, C_6D_{12}): δ 4.6, 9.8 ($SiMe_2$), 22.8, 31.0 (9,9′-C*Me*$_2$), 36.5 (9,9′-*C*Me_2), 97.2 (η⁶-C_6H_6), 122.9, 124.1, 129.6, 134.1, 138.3, 159.0 (xanthene), 201.2 (CO). ^{29}Si{^{1}H} NMR (59.6 MHz, C_6D_{12}): δ 13.3. IR (KBr, cm^{-1}): 1911vs (ν_{CO}).

Reaction of [Ru(xantsil)(CO)(η⁶-toluene)] (1a) with CH_3CN. A suspension of **1a** (150 mg, 0.275 mmol) in acetonitrile (5 mL) was stirred at room temperature for 1 h. Removal of volatiles under vacuum gave a white solid of Ru(xantsil)(CO)$(CH_3CN)_3$ (**2**), which was washed by hexane and dried under vacuum. Yield: 155 mg (98%). Anal. Calcd for $C_{26}H_{33}N_3O_2RuSi_2\cdot CH_3CN$: C, 54.43; H, 5.87; N, 9.07. Found: C, 54.10; H, 5.93; N, 8.65. ^{1}H NMR (300 MHz, CD_3CN, RT): δ 0.407, 0.411 (s, 6H × 2, $SiMe_2$), 1.39, 1.78 (s, 3H × 2, 9-CMe_2), 7.03–7.27 (m, 6H, xanthene). ^{13}C{^{1}H} NMR (75.5 MHz, CD_3CN, 260 K): δ 5.0, 5.1 ($SiMe_2$), 22.7, 30.4 (9-C*Me*$_2$), 36.4 (9-*C*Me_2), 123.0, 123.2, 131.2, 133.2, 138.7, 159.4 (xanthene), 206.0 (CO). ^{29}Si{^{1}H} NMR (59.6 MHz, CD_3CN, 260 K): δ 13.2. IR (KBr, cm^{-1}): 2362w (ν_{CN}), 2336w (ν_{CN}), 1916vs (ν_{CO}), 1389vs, 1254m, 1227s, 1198w, 1125w, 835m, 815m, 777m, 750w. Due to the high lability of acetonitrile ligands, their ^{1}H and ^{13}C NMR signals were not assigned.

Reaction of [Ru(xantsil)(CO)(η⁶-toluene)] (1a) with ᵗBuNC. A Pyrex NMR tube was charged with **1a** (20.0 mg, 0.0366 mmol), ᵗBuNC (14.0 mg, 0.168 mmol), and C_6D_{12} (0.4 mL), and the solution was deaerated by argon for 5 min. The reaction was monitored by ^{1}H NMR spectroscopy. Signals of **1a** were cleanly replaced with those of [Ru(xantsil)(CO)(CNᵗBu)$_3$] (**3**) within 1 h. The solution was slowly concentrated under vacuum to give colorless crystals of **3**. Yield: 21.0 mg (82%). Anal. Calcd for $C_{35}H_{51}O_2Si_2N_3Ru$: C, 59.79; H, 7.31; N, 5.98. Found: C, 59.80; H, 7.28; N, 5.91. MS (EI, 70 eV): *m*/*z* 703 (M^+, 5), 675 (M^+ − CO, 37), 620 (M^+ − CNᵗBu, 84), 593 (M^+ − CO − CNᵗBu, 100). ^{1}H NMR (300 MHz, C_6D_6): δ 0.44 (s, 9H, CNᵗBu *trans* to CO), 1.02 (s, 18H, CNᵗBu *cis* to CO), 1.05, 1.28 (s, 6H × 2, $SiMe_2$), 1.54, 1.67 (s, 3H × 2, 9,9′-CMe_2), 7.18–7.69 (m, 6H, xanthene). ^{13}C{^{1}H} NMR (121.5 MHz, C_6D_6): δ 7.0, 8.8 ($SiMe_2$), 24.5, 30.4 (CN*C*$(CH_3)_3$), 29.8, 30.1 (CNC(*C*H_3)$_3$), 36.4, 55.6 (9,9′-C*Me*$_2$), 55.3 (9,9′-*C*Me_2), 122.9, 124.4, 131.0, 133.2, 139.7, 159.5 (xanthene), 151.1 (*C*NC$(CH_3)_3$), 205.4 (CO). Only one ^{13}C NMR signal assignable to the *C*NᵗBu_3 ligands was found probably due to accidental overlap of the second signal with other signals or its low intensity.

Reaction of [Ru(xantsil)(CO)(η⁶-toluene)] (1a) with PMe_3. A Pyrex tube (10 mm o.d.) was charged with **1a** (20.0 mg, 0.0366 mmol), PMe_3 (22.0 mg, 0.289 mmol), and CH_2Cl_2 (0.5 mL) and connected to a vacuum line. The reaction mixture immediately turned yellow accompanied by the formation of colorless crystals of [Ru(xantsil)(CO)$(PMe_3)_3$] (**4**). The tube was flame-sealed and opened in a glovebox. The mother liquor was decanted and stored at −35 °C to give more crystals of **4**. The crystals were washed with hexane and dried under vacuum. Yield: 21.0 mg (84%). ^{1}H and ^{31}P NMR data were collected in the presence of free PMe_3. ^{13}C and ^{29}Si NMR spectral data could not be obtained due to the low solubility of **4** in organic solvents. Anal. Calcd for $C_{29}H_{51}O_2P_3RuSi_2$: C, 51.08; H, 7.54. Found: C, 50.53; H, 7.40. MS (EI, 70 eV): *m*/*z* 530 (M^+ − 2PMe_3, 8), 502 (M^+ − 2PMe_3 − CO, 17), 325 (100). ^{1}H NMR (300 MHz, CD_2Cl_2): δ 0.53, 0.62 (s, 6H × 2, $SiMe_2$), 1.31, 1.71 (s, 3H × 2, 9,9′-C*Me*$_2$), 1.34 (br., 18H, 2PMe_3 *cis* to CO), 1.47 (d, 9H, $^2J_{PH}$ = 6.7 Hz, PMe_3 *trans* to CO), 6.96–7.21 (m, 6H, xanthene). ^{31}P{^{1}H} NMR (121.5 MHz, CD_2Cl_2): δ −19.5 (d, $^2J_{PP}$ = 36.5 Hz, 2PMe_3 *cis* to CO), −16.2 (t, $^2J_{PP}$ = 36.5 Hz, PMe_3 *trans* to CO). IR (KBr, cm^{-1}): 1932vs (ν_{CO}).

Behavior of 4 in CD_2Cl_2. A Pyrex NMR tube was charged with **4** (15 mg, 0.022 mmol), and CD_2Cl_2 (0.5 mL) was introduced into this tube under high vacuum by the trap-to-trap transfer technique. The colorless solution immediately turned yellow. The yellow solution displayed the ^{1}H and ^{31}P NMR signals of **4**, [Ru(xantsil)-(CO)$(PMe_3)_2$] (**4′**), and free PMe_3. Equilibrium was achieved immediately between **4**, **4′**, and PMe_3 at room temperature. The molar ratio of **4** to **4′** was estimated to be approximately 10:9 based on the intensity ratio of the ^{1}H NMR signals. The NMR tube was opened in a glovebox. Addition of excess PMe_3 into the tube resulted in the formation of a colorless solution containing a single product, **4**. Data for **4′**: ^{1}H NMR (300 MHz, CD_2Cl_2): δ 0.53 (s, 3H × 4, $SiMe_2$), 1.12 (br, 9H, PMe_3), 1.23, 1.66 (s, 3H × 2, 9-CMe_2), 1.44 (br, 9H, PMe_3), 7.05 (m, 2H, xanthene), 7.20 (m, 2H, xanthene), 7.45 (m, 2H, xanthene). ^{31}P{^{1}H} NMR (121.5 MHz, CD_2Cl_2): δ −6.5, 27.4 (br, PMe_3).

Reaction of [Ru(xantsil)(CO)(η⁶-toluene)] (1a) with P^iPr_3. A Pyrex NMR tube was charged with **1a** (5.0 mg, 9.2 μmol) and P^iPr_3 (8.8 μL, 5 equiv), and dichloromethane-d_2 (0.5 mL) was transferred into the tube under vacuum. The tube was flame-sealed. After 30 min at room temperature, the reaction attained equilibrium between **1a** and [Ru(xantsil)(CO)(P^iPr_3)] (**5**) in the molar ratio of 1:1.7. Due to the extremely high lability of P^iPr_3 ligands, isolation of **5** was not achieved even in the presence of excess P^iPr_3. ^{1}H NMR (300 MHz, CD_2Cl_2): δ 0.24, 0.52 (s, 6H × 2, $SiMe_2$), 1.03 (dd, $^3J_{HH}$ = 7.0 Hz, $^3J_{HP}$ = 13.0 Hz, 18H, P(CH*Me*$_2$)$_3$), 1.44, 1.79 (s, 3H × 2, 9-CMe_2), 2.18 (septet, $^3J_{HH}$ = 7.0 Hz, 3H, P(C*H*Me_2)$_3$), 7.14–7.33 (m, 6H, xanthene). ^{31}P{^{1}H} NMR (121.5 MHz, CD_2Cl_2): δ 33.0. ^{29}Si{^{1}H} NMR (59.6 MHz, CD_2Cl_2): 51.8 (d, $^2J_{PSi}$ = 41.8 Hz).

Reaction of [Ru(xantsil)(CO)(η⁶-toluene)] (1a) with PCy_3. A dichloromethane solution (14 mL) of **1a** (100 mg, 0.183 mmol) and PCy_3 (257 mg, 0.916 mmol) was stirred at room temperature in a glovebox. The solution turned from yellow to orange and finally to reddish-orange. After stirring for 30 min, volatiles were removed under reduced pressure. The resulting reddish-orange solid of [Ru(xantsil)(CO)(PCy_3)] (**6**) was washed with hexane three times to remove excess PCy_3 and dried under vacuum. Yield: 102 mg (76%). Anal. Calcd for $C_{38}H_{57}O_2PRuSi_2$: C, 62.17; H, 7.83. Found: C, 61.76; H, 7.98. ^{1}H NMR (300 MHz, CD_2Cl_2): δ 0.20, 0.51 (s, 6H × 2, $SiMe_2$), 0.80–2.01 (m, 33H, PCy_3), 1.51, 1.80 (s, 3H × 2, 9-CMe_2), 7.14–7.36 (m, 6H, xanthene). ^{13}C{^{1}H} NMR (75.5 MHz, CD_2Cl_2): δ 5.44 (d, $^2J_{PC}$ = 5.2 Hz, SiMe), 8.17 (d, $^2J_{PC}$ = 5.2 Hz, SiMe), 23.6, 31.0 (9-C*Me*$_2$), 26.4 (Cy), 27.8 (d, J_{PC} = 9.2 Hz, Cy), 30.7 (Cy), 35.6 (d, J_{PC} = 8.0 Hz, Cy), 37.6 (9-*C*Me_2), 124.2, 125.7, 130.8, 135.7, 136.4, 161.8 (xanthene), 208.0 (d, $^2J_{PC}$ = 3.5 Hz, CO). ^{31}P{^{1}H} NMR (121.5 MHz, CD_2Cl_2): δ 25.0. ^{29}Si{^{1}H} NMR (59.6 MHz, CD_2Cl_2): δ 48.6 (d, $^2J_{PSi}$ = 39.0 Hz), IR (KBr, cm^{-1}): 1876vs (ν_{CO}).

Monitoring the Reaction of [Ru(xantsil)(CO)(PCy_3)] (6) with CO. A Pyrex NMR tube was charged with **6** (7.0 mg, 9.5 μmol) and dichloromethane (0.5 mL). The solution was treated with CO gas (350 μL, 1.6 equiv) via syringe at room temperature and vigorously stirred. The orange solution gradually turned dark green. According to the NMR spectroscopic data, the reaction mixture consists of **6**, [Ru(xantsil)($CO)_2$(PCy_3)] (**7**), and [Ru(xantsil)-($CO)_3$(PCy_3)] (**8**) in the molar ratio of 0.3:1.3:1.0. Due to contamination of **6** and **8**, isolation of **7** was not achieved. Data for **7**: ^{1}H NMR (300 MHz, CD_2Cl_2): δ 0.43 (s, $SiMe_2$). ^{31}P NMR (121.5 MHz, CD_2Cl_2): 37.6. ^{29}Si{^{1}H} NMR (59.6 MHz, CD_2Cl_2): δ 21.8 (d, $^2J_{PSi}$ = 23.2 Hz). IR (CD_2Cl_2, cm^{-1}): 1927vs, 2036vw (ν_{CO}).

Synthesis of [Ru(xantsil)($CO)_3$(PCy_3)] (8). A Schlenk tube was charged with a solution of **6** (75 mg, 0.102 mmol) in CH_2Cl_2 (5 mL), placed in liquid N_2, and evacuated. After filling the tube with CO, the solution was allowed to warm to room temperature and then stirred for 1 h. Volatiles were removed under reduced pressure. The resulting white solid of **8** was washed with hexane three times and dried under vacuum. Yield: 68 mg (84%). Anal. Calcd for $C_{40}H_{57}O_4PRuSi_2$: C, 60.81; H, 7.27. Found: C, 60.45; H, 7.45. ^{1}H NMR (300 MHz, CD_2Cl_2, 230 K): δ 0.46, 0.64, 0.66, 0.72 (s, 3H $\times$ 4, $SiMe_2$), 0.77–2.31 (m, 33H, Cy), 1.29, 1.71 (s, 3H $\times$ 2, 9-CMe_2), 6.93–7.43 (m, 6H, xanthene). ^{13}C{^{1}H} NMR (75.5 MHz, CD_2Cl_2, 200 K): δ 4.84, 6.20, 7.81 (SiMe), 7.11 (d, J_{PC} = 4.2 Hz, SiMe), 13.5, 21.5, 22.2, 35.6 (Cy), 24.8–31.2 (m, Cy and 9-C*Me*$_2$), 34.9 (9-*C*Me_2), 40.8–41.5 (Cy), 121.7, 121.8, 123.2, 123.4, 130.2, 131.1, 131.3, 132.1, 132.9, 156.5, 156.7 (xanthene), 197.6, 203.8, 204.5 (br, CO). ^{31}P{^{1}H} NMR (121.5 MHz, CD_2Cl_2): δ 39.3. ^{29}Si{^{1}H} NMR (59.6 MHz, CD_2Cl_2, 230 K): δ −6.2 (d, $^2J_{PSi}$ = 45.1 Hz, Si *trans* to PCy_3), −2.2 (d, $^2J_{PSi}$ = 8.8 Hz, Si *trans* to CO). IR (KBr, cm^{-1}): 2040vs, 1992vs, 1946vs (ν_{CO}).

Thermolysis of [Ru(xantsil)(CO)(η^6-$C_6H_5CH_3$)] (1a) in *n*-Decane. Complex **1a** (10.0 mg, 0.0183 mmol) and *n*-decane (1.0 mL) were placed in a Pyrex tube, which was flame-sealed under high vacuum. The sample was heated at 140 °C in an oil bath for 1 day. Fine crystals precipitated and the solution became light brown in color. The tube was opened inside the glovebox, and the mother liquor was decanted. The yellow crystals of [Ru(xantsil)$(CO)]_2$ (**9**) were washed with hexane and dried under vacuum. Yield: 6.0 mg (72%). Due to the poor solubility of **9** in organic solvents, no NMR data were available. No acceptable data for elemental analysis were obtained because **9** cannot be purified due to its poor solubility. IR (KBr, cm^{-1}): 1913 (ν_{CO}). Mass (EI, 70 eV): *m*/*z* 908 (M^+, 29), 396 ($M^+/2$ − $SiMe_2$, 23), 381 ($M^+/2$ − $SiMe_2$ − Me, 100).

X-ray Crystal Structure Determination. Crystals of **2**·CH_3CN, **4**, **6**, **8**·CH_2Cl_2, and **9** were mounted at the end of a glass fiber for analysis using a Rigaku RAXIS-RAPID imaging plate diffractometer with graphite-monochromated Mo Kα radiation. Data were collected at 150 K to a maximum 2θ value of 55.0°. Empirical or numerical absorption correction was applied, and the data were corrected for Lorentz and polarization effects. The structure was solved by direct methods and refined by full matrix least-squares techniques on all F^2 data (SHELXL-97).[15] The non-hydrogen atoms were refined anisotropically, and hydrogen atoms were located on idealized positions and refined using a restricted riding model. Selected crystallographic data are listed in Table 1.

Table 2. Selected Interatomic Distances (Å) and Angles (deg) in 4a−c

	4a	4b	4c
Ru−Si1	2.396	2.592	2.512
Ru−Si2	2.498	2.471	2.455
Ru−P1	2.437	2.492	2.482
Ru−P2	2.457	2.256	2.282
Ru−C1	1.857	1.890	1.900
Ru−O1	3.671	3.351	2.300
Si1−Ru−Si2	98.2	98.9	97.8
Si1−Ru−P1	98.6	90.0	91.4
Si1−Ru−P2	96.2	91.1	92.0
Si1−Ru−C1	89.5	175.0	172.0
Si2−Ru−P1	160.7	159.2	164.8
Si2−Ru−P2	93.0	91.1	93.3
Si2−Ru−C1	83.5	108.1	76.4
P1−Ru−P2	94.6	108.1	98.6
P1−Ru−C1	87.1	88.3	86.1
P2−Ru−C1	173.7	98.2	95.9
Si1−Ru−O1			83.1
Si2−Ru−O1			78.7
C1−Ru−O1			96.1
P2−Ru−O1			164.6

Acknowledgment. This work was supported by Grants-in-Aid for Scientific Research (Nos. 18064003 and 18350027) from the Ministry of Education, Culture, Sports, Science and Technology of Japan.

Supporting Information Available: A preliminary X-ray structure analysis of **3** in PDF format. Crystallographic data in CIF format for **2**·CH_3CN, **4**, **6**, **8**·CH_2Cl_2, and **9**. These materials are available free of charge via the Internet at http://pubs.acs.org.

OM701194E

(15) (a) Sheldrick, G. M. *SHELXS-97*, Programs for Solving X-ray Crystal Structures; University of Göttingen, 1997. (b) Sheldrick, G. M. *SHELXL-97*, Programs for Refining X-ray Crystal Structures; University of Göttingen, 1997.